19 Application of Novel Nanoporous Sorbents for the Removal of Heavy Metals, Metalloids, and Radionuclides

Shas V. Mattigod, Glen E. Fryxell, Kent E. Parker, and Yuehe Lin

CONTENTS

ABSTRACT

A new class of hybrid nanoporous materials for removing toxic heavy metals, oxyanions, and radionuclides from aqueous waste streams has been developed at the Pacific Northwest National Laboratory. These novel materials consist of functional molecules such as thiols, ethylenediamine-complexed copper, and carbamoylphosphonates that are self-assembled as monolayers within the nanopores of a synthetic silica-based material. Tests indicated that these sorbents (self-assembled monolayers on mesoporous silica — SAMMS) can achieve very high sorbate loadings (~6 meq/g) very rapidly with relatively high specificity (K_d: 1×10^8 ml/g). Because of the specifically tunable nature of the functionalities, these nanoporous sorbents can be targeted to remove a selected category of contaminants such as heavy metals (Ag, Cd, Cu, Hg, and Pb), oxyanions (As and Cr), and radionuclides (^{137}Cs, ^{129}I, ^{237}Np, and isotopes of Pu, Th, and U) from waste streams.

19.1 INTRODUCTION

Successful synthesis of silica-based nanoporous materials using liquid crystal templating was achieved about a decade ago [1,2]. Since then, use of these nanoporous materials in diverse applications such as catalysis, sensor technology, and sorbents has proved to be feasible. In sorbent technology applications, the nanoporous materials offer a significant advantage over conventional

sorbents, due to their high surface areas (~500 to 1000 m^2/g). However, the pore surfaces of these novel materials need to be activated before they can be deployed as effective sorbents.

Typically, the nanoporous materials are synthesized through a combination of oxide precursors and surfactant molecules in solution reacted under mild hydrothermal conditions. Under these conditions, the surfactant molecules form hexagonally ordered rod-like micelles, and the oxide materials precipitate on these micellar surfaces to replicate the organic templates formed by the rod-like micelles. Subsequent calcination at 500°C removes the surfactant templates and leaves a high surface area nanoporous ceramic substrate. The pore size of these ceramic substrates can be controlled by using surfactants of different chain lengths.

The authors have developed a method to activate the pore surfaces of silica-based nanoporous materials so that these materials can be used as effective sorbents. This process consists of synthesizing, within pores, self-assembled monolayers of adsorptive functional groups selected to adsorb specific groups of contaminants. Molecular self-assembly is a unique phenomenon in which functional molecules aggregate on an active surface, resulting in an organized assembly that has order and orientation.

In this approach, bifunctional molecules containing a hydrophilic head group and a hydrophobic tail group adsorb onto a substrate or an interface as closely packed monolayers (Figure 19.1). The driving forces for the self-assembly are the intermolecular interactions between the functional molecules (such as van der Waals forces). The tail group and the head group can be chemically modified to contain certain functional groups to promote covalent bonding between the functional organic molecules and the substrate on one end, and the molecular bonding between the organic molecules and the metals on the other. For instance, populating the head group with alkylthiols (which are well known to have a high affinity for various soft heavy metals, including mercury) results in a functional monolayer that specifically adsorbs heavy metals such as Ag, Cd, Cu, Hg, and Pb.

If the head group consists of Cu-ethylenediamine complex, the monolayer will sorb oxyanions (As, Cr, Se, Mo) with high specificity. Additional monolayers with head groups designed by the authors include acetamide and propinamide phosphonates for binding actinides (Am, Pu, U, Th); Hg- and Ag-thiol for sorbing radioiodine; and a ferricyanide Cu-EDA complex for selectively bonding radiocesium. The functionalized monolayer and substrate composite (Figure 19.1) was designated as SAMMS. Various self-assembled monolayer functionalities and the contaminants that they were designed to target are shown in Figure 19.2.

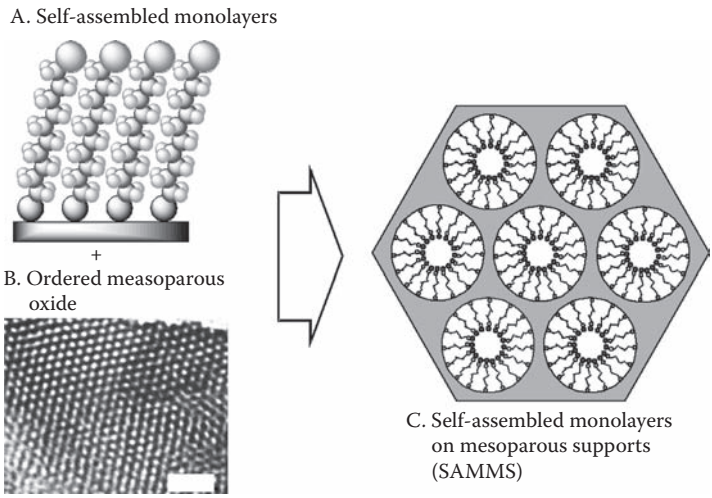

FIGURE 19.1 Technological basis of novel nanoporous sorbents.

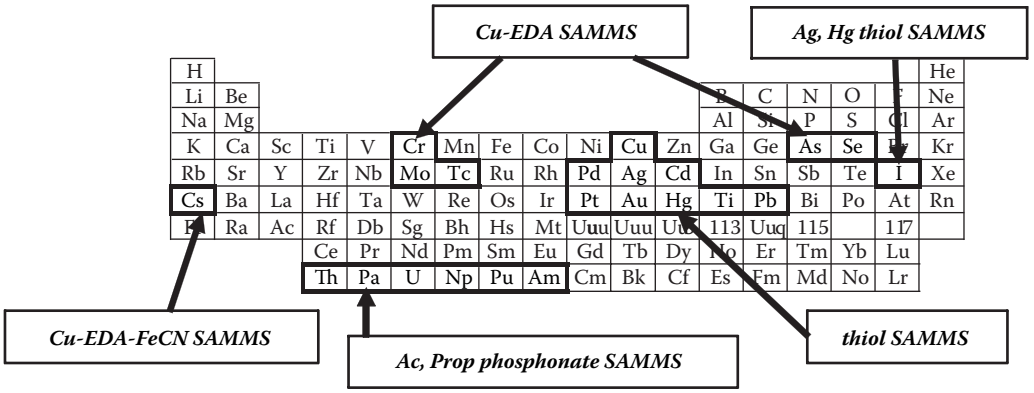

FIGURE 19.2 SAMMS technology and the targeted contaminant groups.

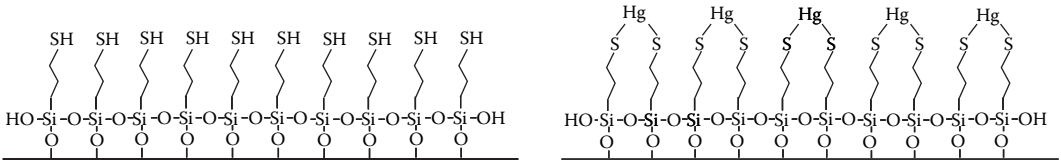

FIGURE 19.3 Schematic conformation of thiol-functionalized monolayers (left) and the bidentate bonding of mercury to the thiol moieties (right).

19.2 MATERIALS AND METHODS

19.2.1 Synthesis of Self-Assembled Monolayers

The nanoporous silica substrate was prepared using cetyltrimethylammonium chloride/hydroxide as the template and silicate and mesilyletene solutions as the reactants. Following hydrothermal reaction at 105°C for 1 week, the product was washed, dried, and calcinated at 580°C for 12 h to remove the template. The resulting nanoporous material had a surface area of 900 m^2/g with an average pore size of 5.5 nm in diameter. The details of the substrate synthesis are provided by Feng et al. [3].

The thiol-functionalized SAMMS was synthesized by using trismethoxymercaptopropylsilane and allowing the molecular self-assembly to occur on the pore surface of the silica substrate in a toluene suspension [3]. The resulting monolayer had cross-linked silanes bonded to the pore surface with exposed thiol head groups (Figure 19.3) with a functional surface density of 6.2 silanes/nm^2. Similarly, Cu-EDA SAMMS was generated by a monolayer of EDA-terminated silane [2-amino-ethyl-3-aminopropyl trimethoxysilane], which was saturated with copper [4] (Figure 19.4). The surface population of this functionality was calculated to be 4.9 silanes/nm^2.

For radiocesium removal, the Cu-EDA FeCN SAMMS was synthesized from the Cu EDA SAMMS form by saturating the Cu sites with ferricyanide ions [5] (Figure 19.5). Actinide-adsorbing SAMMS was prepared by monolayer grafting of carbamoylphosphonate (CMPO) silanes (acetamide and propionaminde phosphonate silanes) [6] (Figure 19.6). The resulting SAMMS materials (APH SAMMS and PPH SAMMS, respectively) had functional densities of 2.2 to 2.4 silanes/nm^2 as measured by solid state ^{29}Si nuclear magnetic resonance (NMR) spectrometry [7].

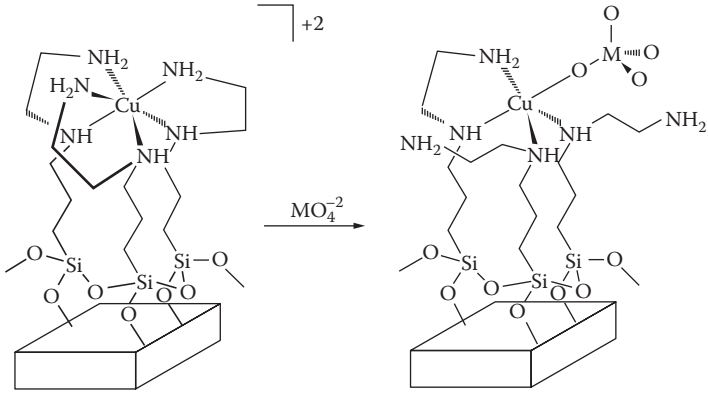

FIGURE 19.4 Schematic of copper ethylenediamine functionality (left) and the tetrahedral oxyanion binding mechanism (right).

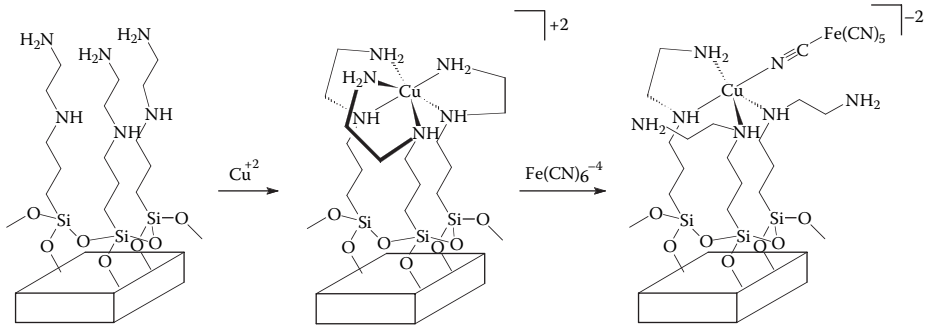

FIGURE 19.5 Sequence of synthesis of ferricyanide Cu-EDA SAMMS (right) starting with EDA SAMMS (left) and Cu-EDA SAMMS (middle).

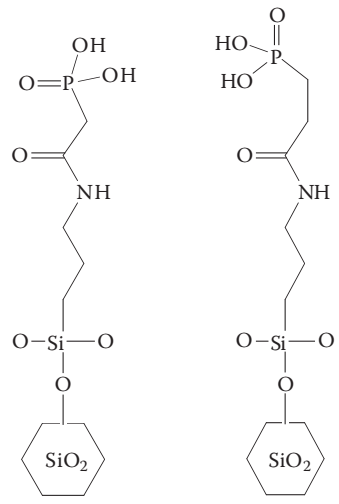

FIGURE 19.6 Schematic structures of acetamide and propinamide phosphonate SAMMS.

19.3 ADSORPTION EXPERIMENTS

Heavy metal adsorptive properties of thiol-SAMMS was tested by contacting known quantities of sorbent with a fixed volume of 0.1 *M* $NaNO_3$ solution containing the metal of interest (Ag, Cd, Cu, Hg, and Pb). The initial concentrations of these metals ranged from 0.05 to 12.5 meq/L and the solution-to-sorbent ratio in these experiments ranged from ~200 to 5000 ml/g. The suspensions were continually shaken and allowed to react under ambient temperature conditions (~25°C) for approximately 8 h. Next, the sorbent and the contact solutions were separated by filtration and the residual metal concentrations in aliquots were measured by using inductively coupled plasma mass spectrometry (ICP-MS).

Kinetics of adsorption of mercury by thiol-SAMMS was tested by contacting 200 mg of sorbent with 500 mL of 0.1 *M* $NaNO_3$ solution spiked with 0.1 meq/L concentration of mercury. The mixture was stirred constantly, and periodically aliquots of solution were drawn to monitor the residual mercury concentration. For comparison, mercury adsorption kinetic performance of a resin (GT-73) was also studied.

Experiments to evaluate the radioiodine adsorption performance of Hg-thiol and Ag-thiol SAMMS were conducted by equilibrating sorbent samples with aliquots of groundwater spiked with 3.65×10^7 bq/L of ^{125}I (Table 19.1). Solution-to-sorbent ratios ranging from 100 to 10,000 mL/g were used to evaluate the degree of ^{125}I loading on these materials. The mixture was gently agitated for ~20 h at 25 ± 3°C and portions of equilibrated solutions were filtered and counted for residual ^{125}I activity. Analysis of ^{125}I in liquid samples was conducted by gamma-ray spectrometry, using a calibrated Wallac® 1480 Wizard™ 3-in. NaI detector with built-in software.

Oxyanion adsorption characteristic of Cu-EDA SAMMS was evaluated by contacting the sorbent with 3 meq/L of Na_2SO_4 solution containing either chromate (~0.02 to 18 meq/L) or arsenate (~0.01 to 29 meq/L) ions. Solution to sorbent ratio in these experiments ranged from 100 to 500 ml/g. After 12 h of contact, filtered aliquots of solution were analyzed by inductively-coupled plasma atomic emission spectrometry (ICP-AES). Adsorption kinetics experiment was conducted by contacting 200 mg of sorbent with 500 mL of groundwater spiked with 0.005 meq/L concentration of arsenate. The mixture was stirred constantly, and periodically aliquots of solution were drawn to monitor the residual arsenate concentration.

The cesium adsorption performance of Cu-EDA FeCN SAMMS was evaluated by contacting 50 mg of the sorbent with 10 mL of solution containing 0.5 to 8.4 meq/L of cesium. After 2 h of reaction, the solution was separated by filtration and the residual concentration of cesium was measured by using ICP-MS. A cesium adsorption kinetics experiment was conducted by contacting

TABLE 19.1
Composition of Groundwater Sample

Constituent	mg/L	Constituent	mg/L
Al	0.01	Alk(CO_3^{2-})	54.1
Ca	49.5	Cl	7.8
Fe	0.07	Br	0.10
K	1.7	F	0.17
Mg	14.6	NO_2	0.68
Mn	0.17	NO_3	27.2
Na	13.2	SO_4	82.5
Si	16.5	pH (SU)	8.1

50 mg of sorbent with 10 mL of cesium solution (0.015 meq/L). Periodically, aliquots of filtered solution were analyzed for cesium concentration by using ICP-MS.

The actinide-specific APH- and PPH-SAMMS were tested by contacting 100 mg quantities of each of these sorbents with 10-mL portions of solutions containing 2×10^6 counts per minute(CPM)/L of Pu(IV) in a matrix of acidified (pH = 1) 1 *M* $NaNO_3$ with separately spiked (0.01 *M*) Pu-complexing ligands such as phosphate, sulfate, ethyelenediaminetetraacetate (EDTA), and citrate. After 1 to 4 h of reaction, the solution was separated by filtration, mixed with Ultima Gold™ scintillation cocktail, and the residual alpha activity of Pu(IV) was measured by using a liquid scintillation counter (2550 TR/AB Packard Instruments, Meriden, Connecticut).

19.4 RESULTS AND DISCUSSION

The data from the adsorption experiments (Figure 19.7 and Table 19.2) indicated that thiol-SAMMS adsorbed the heavy metals with significant affinity. The predicted adsorption maxima were 0.56, 0.72, 1.27, 4.11, and 6.37 meq/g for Cu, Pb, Cd, Ag, and Hg, respectively. The calculated distribution coefficients were 4.6×10^1 to 1.8×10^5; 2.2×10^2 to 8.6×10^3; 2.2×10^2 to 1.9×10^4; 1.2×10^3 to 8.7×10^5; and 1×10^3 to 3.5×10^8 ml/g for Cu, Pb, Cd, Ag, and Hg, respectively.

Such selectivity and affinity in binding these heavy metals by thiol-SAMMS can be explained on the basis of the hard and soft acid base principle (HSAB) [8–10], which predicts that the degree of cation softness directly correlates with the observed strength of interaction with soft base

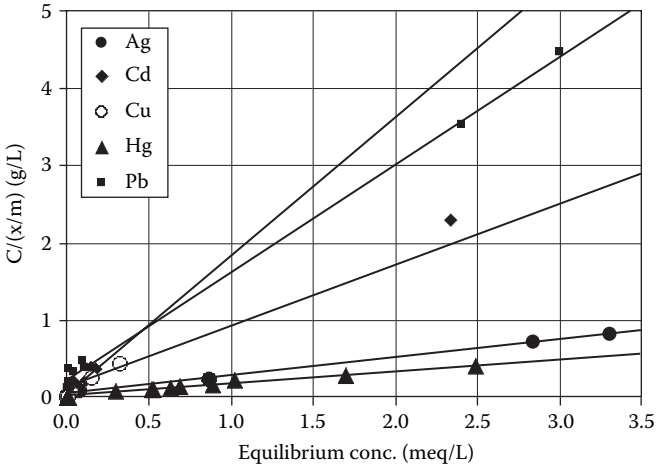

FIGURE 19.7 Langmuir adsorption isotherms for heavy metal adsorption by thiol-SAMMS.

TABLE 19.2
Heavy Metal Adsorption Characteristics of Thiol–SAMMS

Heavy metal	Adsorption maximum (meq/g)	K_d (ml/g)
Ag	4.11	1.2×10^3–8.7×10^5
Cd	1.27	2.2×10^2–1.9×10^4
Cu	0.56	4.6×10^1–1.8×10^5
Hg	6.37	1.0×10^3–3.5×10^8
Pb	0.72	2.2×10^2–8.6×10^3

functionalities such as thiols (–SH groups). According to the HSAB principle, soft cations and anions possess relatively large ionic size, low electronegativity, and high polarizability (highly deformable bonding electron orbitals); therefore, they mutually form strong covalent bonds. The order of adsorption maxima observed in this experiment appears to reflect the order of softness calculated by Misono et al. [11] for these heavy metals.

The kinetics data indicated that thiol-SAMMS adsorbed ~99% of the dissolved mercury within the first 5 min of reaction (Figure 19.8). Comparatively, the resin (GT-73) adsorbed only ~18% of the dissolved mercury during the initial 5 min. These data showed that thiol-SAMMS substrate adsorbs mercury about two to three orders of magnitude faster than the commercial GT-73 ion-exchange resin. After 8 h of reaction, thiol-SAMMS reduced the residual concentration of mercury to ~0.04 mg/L; the resin material was not capable of reducing mercury concentration below 1mg/L. Calculated distribution coefficients (K_d) indicated that thiol-SAMMs adsorbed mercury at about one to three orders of magnitude higher selectivity ($7 \times 10^3 – 3.6 \times 10^5$ ml/g) than the resin material ($4.5 \times 10^2 – 1.9 \times 10^3$ ml/g).

Results from the radioiodine adsorption experiments indicated that Hg-thiol, and Ag-thiol SAMMS very effectively adsorbed ^{125}I from the groundwater matrix (Table 19.3). Both forms of SAMMS exhibited very high distribution coefficients (K_d: 2.9×10^4 to 1.2×10^5 ml/g), indicating that radioiodine was sorbed with high specificity even in the presence of anions in the groundwater that were present in significantly higher concentrations than radioiodine. Such selectivity and

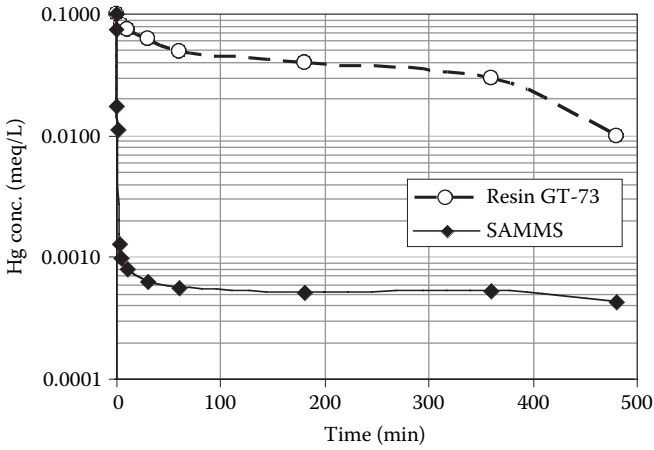

FIGURE 19.8 Kinetics of mercury adsorption by thiol-SAMMS and an ion exchange resin.

TABLE 19.3
Adsorption of Radioiodine (^{125}I) by Ag and Hg Thiol–SAMMS

Eq. activity (Bq/mL)	Ads. density (Bq/g)	K_d (ml/g)	Eq. activity (Bq/mL)	Ads. density (Bq/g)	K_d (ml/g)
	Ag-thiol–SAMMS			Hg-thiol–SAMMS	
108	3.58×10^6	3.31×10^4	611	1.76×10^7	2.88×10^4
409	1.79×10^7	4.38×10^4	942	3.59×10^7	3.81×10^4
848	3.64×10^7	4.29×10^4	1911	1.82×10^8	9.52×10^4
2299	1.73×10^8	7.53×10^4	2801	3.24×10^8	1.16×10^5
2961	3.50×10^8	1.18×10^5			

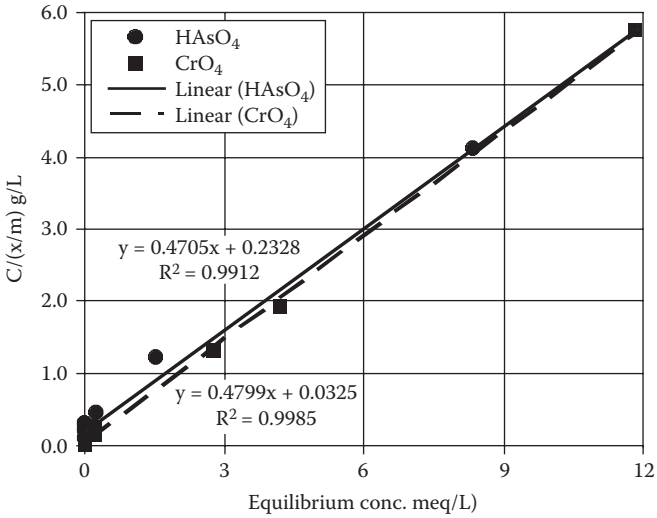

FIGURE 19.9 Langmuir adsorption isotherms for arsenate and chromate by Cu-EDA SAMMS.

affinity in binding of ^{125}I is because iodine is a much softer base than other anions and would bond preferentially to very soft cations — namely, Ag and Hg.

Results of the arsenate and chromate adsorption tests indicated that Cu-EDA SAMMS very effectively adsorbed both these oxyanions from Na_2SO_4 solution. The predicted adsorption maxima from the Langmuirian fit to the data were 2.13 and 2.08 meq/g for arsenate ($HAsO_4$) and chromate (CrO_4), respectively (Figure 19.9). The calculated distribution coefficients were 2.4×10^2 to 1.0×10^4 and 1.7×10^2 to 1.0×10^6 ml/g for arsenate and chromate, respectively. The bonding mechanism of these oxyanions was studied by Kelly et al. [12,13] using x-ray adsorption fine spectroscopy (XAFS), which indicated that bonding was monodentate in nature. The copper ion was bonded directly to the oxyanion by a shared oxygen. The adsorption process changed the coordination of copper from octahedreal to trigonal bipyramidal geometry. The bonding did not alter the tetrahedral symmetry of $HAsO_4$ ion, but the symmetry of the CrO_4 ion was distorted with two short and two long Cr–O bond distances.

The data from the kinetic experiment (Figure 19.10) showed that, within the first 2 min, about 98% of the arsenate was removed by Cu-EDA SAMMS. The adsorption was remarkably fast and the reaction reached a steady state in about 60 min. The residual concentration of arsenate was 2.03×10^{-5} meq/L (~0.8 ppb) — well below the EPA-proposed new regulatory limit (10 ppb) for arsenic in drinking water.

The data from the adsorption experiments indicated that Cu-EDA FeCN SAMMS adsorbed cesium with significant affinity (Figure 19.11). The predicted adsorption maximum was 1.34 meq/g compared to the measured value of 1.33 meq/g. Both these loading values are close to the theoretical maximum adsorption capacity of 1.5 meq/g calculated for this form of SAMMS material. Although the initial solution contained one to two orders of magnitude excess of Na than Cs, the calculated distribution coefficients ranging from 7.7×10^2 to 4.8×10^4 ml/g indicated that Cs bonded preferentially to the FeCN sites. The observed selectivity of ferrocyanide ligand for Cs confirms the previous observations of preferred bonding of this ligand with Cs than with other alkali earth cations [14,15].

The data from the adsorption kinetics experiment indicated very rapid binding of cesium by the Cu-EDA FeCN SAMMS (Figure 19.12). About 99.8% of the cesium present in solution was adsorbed, reducing the residual dissolved concentration to $<3 \times E -5$ meg/L within 1 min of contact

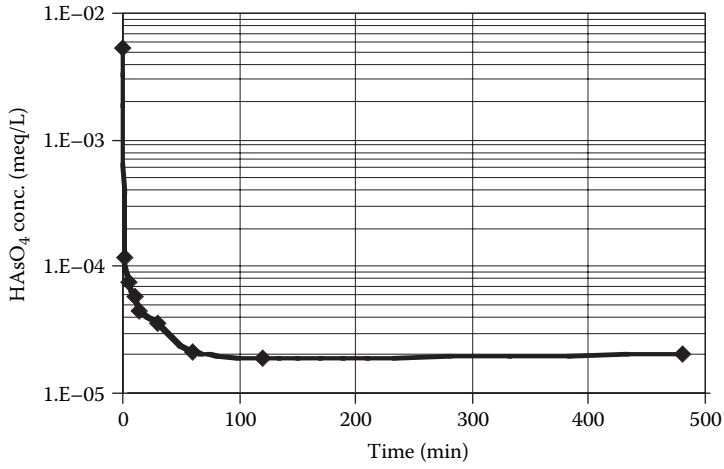

FIGURE 19.10 Kinetics of arsenate adsorption by Cu-EDA-SAMMS.

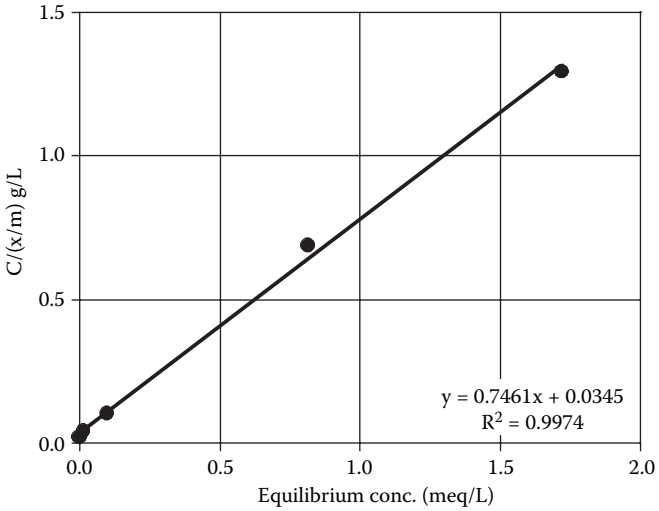

FIGURE 19.11 Langmuir adsorption isotherms for cesium by Cu-EDA FeCN SAMMS.

time. Bulk of the Cs adsorption (99.96%) had occurred within 20 min, resulting in very low residual concentrations of ~6.4×10^{-6} meq/L (0.85 ppb).

Plutonium adsorption data (Table 19.4) indicated that APH and PPH SAMMS adsorbed this actinide with high specificity (K_d: 1.7×10^4 to 2.1×10^4 ml/g). However, on average, APH SAMMS performed slightly better in adsorbing Pu(IV) from solution. In this experiment, the presence of complexants with differing chelating strengths did not significantly affect Pu(IV) adsorption by these nanoporous sorbents. Considering that the complexation constants of Pu(IV) with these ligands vary in the order EDTA > citrate > phosphate >> sulfate > nitrate [16], very high adsorption affinity shown by these sorbents indicates that the CMPO ligand (APH and PPH) functionality-based adsorption substrates are capable of chelating Pu(IV) much more strongly than these ligands. Additionally, the APH SAMMS has been shown to adsorb Pu(IV) very rapidly with bulk of the sorbate removed from solution in under 1 min [17].

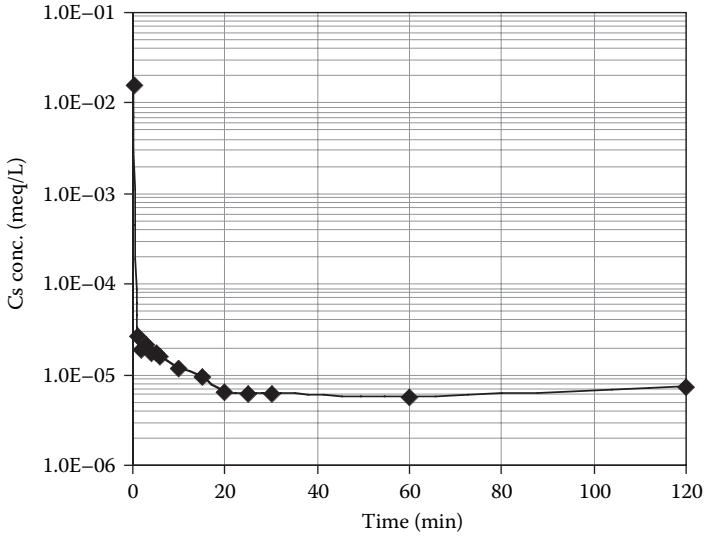

FIGURE 19.12 Kinetics of cesium adsorption by Cu-EDA FeCN SAMMS.

TABLE 19.4
Adsorption of Pu(IV) by APH– and PPH–SAMMS

Ligand	APH SAMMS	PPH SAMMS
	K_d (ml/g)	
Nitrate	2.12×10^4	1.58×10^4
Nitrate + phosphate	2.04×10^4	1.75×10^4
Nitrate + sulfate	1.98×10^4	1.82×10^4
Nitrate + EDTA	2.05×10^4	1.56×10^4
Nitrate + citrate	2.31×10^4	1.87×10^4

19.5 SUMMARY AND CONCLUSIONS

A new class of hybrid nanoporous materials has been developed for removing toxic heavy metals, oxyanions, and radionuclides from aqueous waste streams. Tests showed that thiol-SAMMS designed for heavy metal adsorption showed significant loading (0.56 to 6.37 meq/g) and high selectivity (K_d: 4.6×10^1 to 3.5×10^8 ml/g) for contaminants such as Cu, Pb, Cd, Ag, and Hg.

Results of the arsenate and chromate adsorption tests indicated that Cu-EDA SAMMS very effectively adsorbed both these oxyanions with predicted adsorption maxima of ~2.1 meq/g, with distribution coefficient ranging from 1.7×10^2 to 1.0×10^6 ml/g. Adsorption experiments conducted using Ag- and Hg-capped thiol SAMMS sorbents very effectively adsorbed ^{125}I from a groundwater matrix. Both forms of thiol-SAMMS exhibited very high distribution coefficients (K_d: 2.9×10^4 to 1.2×10^5 ml/g), indicating that radioiodine was sorbed with high specificity even in the presence of anions in the groundwater that were present in significantly higher concentrations than radioiodine.

Another sorbent, designed to adsorb radiocesium (Cu-EDA FeCN SAMMS) specifically, when tested exhibited loading as high as 1.33 meq/g and distribution coefficients ranging from

7.7×10^2 to 4.8×10^4 ml/g. Tests conducted using carbamoylphosphonate-functionalized nanoporous substrates (APH and PPH SAMMS) showed that these sorbents very effectively adsorbed Pu(IV) from solutions containing complexing ligands, such as EDTA, citrate, phosphate, sulfate, and nitrate. Distribution coefficients as high as 2×10^4 ml/g confirmed that the CMPO-based functionalities assembled on nanoporous substrates are very effective scavengers for actinide ions such as Pu.

Self-assembled monolayers of selected functionalities on nanoporous silica substrates can achieve very high sorbate loadings very rapidly with relatively high specificities. These novel classes of sorbent materials therefore will be very effective in removing a wide range of targeted contaminants from waste streams.

ACKNOWLEDGMENTS

This study was supported by the Office of Science/Office of Biological and Environmental Research of the U.S. Department of Energy and the IR&D funds from Battelle. Pacific Northwest National Laboratory is operated for the U.S. Department of Energy by Battelle under contract DE-AC06-76RLO 1830.

REFERENCES

1. Beck, J.S., J.C. Vartuli, W.J. Roth, M.E. Leonowicz, C.T. Kresge, K.D. Schmitt, C.T-W. Chu, D.H. Olson, E.W. Sheppard, S.B. McCullen, J.B. Higgins, and J.L. Schlenker. A new family of mesoporous molecular sieves prepared with liquid crystal templates. *J. Am. Chem. Soc.* 114, 10834–10843, 1992.
2. Kresge, C.T., M.E. Leonowicz, W.J. Roth, J.C. Vartuli, and J.S. Beck. Ordered mesoporous molecular sieves synthesized by a liquid crystal template mechanism. *Nature* 359, 710–712, 1992.
3. Feng, X., G.E. Fryxell, L.Q. Wang, A.Y. Kim, J. Liu, and K.M. Kemner. Functionalized monolayers on ordered mesoporous supports. *Science.* 276, 865, 1997.
4. Fryxell, G.E., J. Liu, A.A. Hauser, Z. Nie, K.F. Ferris, S.V. Mattigod, M. Gong, and R.T. Hallen. Design and synthesis of selective mesoporous anion traps, *Chem. Mater.* 11, 2148–2154, 1999.
5. Lin Y., G.E. Fryxell, H. Wu, and M. Engelhard. Selective sorption of cesium using self-assembled monolayers on mesoporous supports. *Env. Sci. Technol.* 35, 3962–3966, 2001.
6. Birnbaum, J.C., B. Busche, Y. Lin, W.J. Shaw, and G.E. Fryxell. Synthesis of carbamoyl-phosphonate silanes for the selective sequestration of actinides. *Chem. Commun.* 1374–1375, 2002.
7. Yantasee, W.Y. Lin, Y., G.E. Fryxell, B.J. Busche, and J.C. Birnbaum. Removal of heavy metals from aqueous solution using novel nanoengineered sorbents: self-assembled carbamoylphosphonic acids on mesoporous silica. *Sep. Sci. Tech.* 15, 3809–3825, 2003.
8. Pearson, R.G., Hard and soft acids and bases part 1, *J. Chem. Educ.* 45, 581–587, 1968.
9. Pearson, R.G. Hard and soft acids and bases part 2, *J. Chem. Educ.* 45, 643–648, 1968.
10. Hancock, R.D. and A.E. Martell. Hard and soft acid and base behavior in aqueous solution: steric effects make some metal ions hard: a quantitative scale of hardness-softness for acids and bases. *J. Chem. Educ.* 74, 644, 1996.
11. Misono, M., E. Ochiai, Y. Saito, and Y. Yoneda. A dual parameter scale for the strength of Lewis acids and bases with the evaluation of their softness. *J. Inorg. Nucl. Chem.* 29, 2685–2691, 1967.
12. Kelly, S., K. Kemner, G.S. Fryxell, J. Liu, S.V. Mattigod, and K.F. Ferris. An x-ray absorption fine structure spectroscopy determination of the binding mechanisms of tetrahedral anions to self-assembled monolayers on mesoporous supports. *J. Synchrotron Rad.* 8, 922–924, 2001.
13. Kelly, S., K. Kemner, G.E. Fryxell, J. Liu, S.V. Mattigod, and K.F. Ferris. X-ray absorption fine structure spectroscopy study of the interactions between contaminant tetrahedral anions to self-assembled monolayers on mesoporous supports. *J. Phys Chem.* 105, 6337–6346, 2001.
14. Mekhail, F.M. and K. Benyamin. Sorption of cesium on zinc hexacyanoferrate(III), zinc hexacyanoferrate(III) and hexacyanocobaltate(III). *Radiochim. Acta.* 55, 95–99, 1991.

15. Ayers, J.B. and W. H. Waggoner. Synthesis and properties of two series of heavy metal hexacyanoferrates. *J. Inorg Nucl Chem.* 33, 721, 1971.
16. Cleveland, J.M. *The Chemistry of Plutonium,* American Nuclear Society, LaGrange Park, IL, 1979.
17. Fryxell, G.E., Y. Lin, and H. Wu. Environmental applications of self-assembled monolayers on mesoporous supports (SAMMS). *Stud. Surf. Sci. Cat.* 141, 583–589, 2002.